HHS Public Access

Author manuscript

Nat Struct Mol Biol. Author manuscript; available in PMC 2015 April 01.

Published in final edited form as:

Nat Struct Mol Biol. 2014 October ; 21(10): 937–943. doi:10.1038/nsmb.2887.

Multiple *in vivo* pathways for *E. coli* small ribosomal subunit assembly occur on one pre-rRNA

Neha Gupta[1] and **Gloria M Culver**[1,2]

[1]Department of Biology, University of Rochester, Rochester, New York 14627, USA

[2]Center for RNA Biology, University of Rochester, Rochester, New York 14627, USA

Abstract

Processing of transcribed precursor ribosomal RNA (pre-rRNA) to a mature state is a conserved aspect of ribosome biogenesis *in vivo*. We developed an affinity purification system to isolate and analyze *in vivo* formed pre-rRNA containing ribonucleoprotein particles (rRNPs) from wild-type *E. coli*. We observed that the first processing intermediate of pre-SSU rRNA is a platform for biogenesis. These pre-SSU containing RNPs have differing ribosomal protein and auxiliary factors association and rRNA folding. Each RNP lacks the proper architecture in functional regions suggesting that checkpoints preclude immature subunits from entering the translational cycle. This work offers *in vivo* snapshots of SSU biogenesis and reveals that multiple pathways exist for the entire SSU biogenesis process in wild-type *E. coli*. These findings have important implications in understanding SSU biogenesis *in vivo* and offer a general strategy for analysis of RNP biogenesis.

Introduction

Ribosome biogenesis, production of mature ribosomal subunits, is indispensable and essential in all living organisms. Ribosome biogenesis involves proper coordination of transcription, processing, modification and structural rearrangement of ribosomal RNA (rRNA), ribosomal protein (r-protein) synthesis, modification and association with rRNA, to form functional ribonucleoprotein complexes (RNPs)[1]. The process of forming mature rRNA by the action of several nucleases on precursor rRNA (pre-rRNA) is conserved in all domains of life; while these events in eukaryotes have been studied in detail[2], such studies in prokaryotes have been lacking. This lack of knowledge hampers not only understanding of an essential cellular process but also, as changes in bacterial ribosome biogenesis have recently been linked to altered virulence and drug resistance in pathogens[3–6], understanding this process is of particular importance in the discovery of new antimicrobials[7].

Correspondence to: Gloria M Culver.

Author contributions

N.G. and G.M.C designed the study and experiments and wrote the manuscript; N.G. performed experiments and analyzed the data.

Competing financial interests

The authors declare no competing financial interests.

Like most cellular RNAs, rRNAs are transcribed as a primary transcript, which undergoes maturation to a functional state[8]. In all domains of life, a primary rRNA transcript is processed to release fragments containing the individual rRNA species. Early pre-rRNA species contain mature rRNA sequences and additional spacer sequences at both ends (5′ and 3′)[9]. In *E. coli*, seven rDNA operons encode the three rRNAs [16S (SSU), 23S (Large subunit or LSU) and 5S (LSU) rRNAs]. Ribonuclease (RNase) III (a double stranded endonuclease) cleavage is believed to be the first step in the release of pre-rRNAs[10,11]. RNase III action on pre-16S rRNA resolves a pre-rRNA product,17S rRNA, with 115 nucleotides upstream of the mature 5′ end (Leader) and 33 nucleotides downstream of the mature 3′ end (Trailer) (see Fig. 1a)[12]. 5′ end maturation involves two cleavage events catalyzed by RNases E and G[13,14]. Maturation of the 3′ end of 16S rRNA is less well understood as several distinct RNases have been linked to this process[15,16]. Thus, while 16S rRNA maturation enzymes and the length of pre-rRNA processing intermediates have been identified, substrates, timing of enzyme action and coupling of 16S rRNA maturation to other SSU biogenesis events are not well understood.

An integrated understanding of critical *in vivo* bacterial ribosome biogenesis events is still lacking after nearly five decades of study. Mutant strains and chemical perturbations have yielded some information on the SSU biogenesis pathway and intermediates in *E. coli*[17–19]. Small populations of ribosomes undergoing biogenesis (2–5%), rapid kinetics and asynchronous transcription from rDNA loci greatly complicates identification and characterization of bacterial SSU biogenesis intermediates[20]. To overcome these deficiencies, we developed an RNA tagging and affinity purification system to isolate SSU assembly intermediates from the wild-type cells. This system allowed purification of SSU intermediates, which were essentially free of contaminating mature SSUs, thus allowing detailed characterization of the pre-SSUs. One pre-SSU rRNA (17S rRNA) was the predominant species associated with all purified assembly intermediates. Yet, these 17S rRNA containing RNPs had distinct rRNA architectures and protein composition. These findings suggest that distinct RNPs form on a 17S rRNA platform during SSU biogenesis *in vivo* and that different SSU biogenesis snapshots can be characterized using this strategy. While each pre-SSU RNP was distinct, they lacked mature architecture at several functional sites, thus indicating preclusion of pre-rRNPs from involvement in translation. Several independent pathways for maturation of 17S rRNA in these RNPs were observed suggesting that flux through SSU biogenesis involves multiple pathways. Additionally, these data suggest that similar analysis will be productive with most dynamic cellular RNPs.

Results

Purification of SSU assembly intermediates formed *in vivo*

We devised a strategy for purification of pre-16S rRNA containing SSU assembly intermediates using a MS2 bacteriophage RNA stem loop (hereafter referred to as MS2 tag) at different positions in the pre-16S rRNA transcribed spacers[21]. We examined several different locations for insertion of the MS2 tag in this study; the nomenclature is based on the nucleotide of tag insertion site with an L (Leader) or T (Trailer): for example, 105L is

105 nucleotides into the Leader sequence (Fig. 1b). As a control and comparison, a tag at position 86 in mature 16S rRNA (86M) was used to isolate mature SSUs[22].

As disruption of ribosome biogenesis or rRNA maturation can result in slow growth and cold sensitivity[18,23], we determined if the MS2 tag insertions effected growth and therefore by extension SSU biogenesis. The three MS2 rDNA tagged plasmids (105L, 11L and 20T), as the sole copy of rDNA in an *E. coli* strain lacking all chromosomal rDNA copies[24], were able to complement growth at levels indistinguishable from wild-type, non-tagged constructs. These results indicate that insertion of these tags does not affect ribosome biogenesis (Fig. 1c). A second independent *in vivo* assay demonstrated that expression of 105L, 11L and 20T tagged rDNA plasmids did not affect growth at non-permissive temperatures; thus, these MS2 tagged rRNAs do not result in cold-sensitivity, a hallmark of ribosome biogenesis defects (Supplementary Fig. 1b). In contrast, an rDNA plasmid with an MS2 tag at position 86L exhibited cold-sensitivity; this result indicates that defects associated with MS2 tagging of pre-16S rRNA can be observed in our assay but given this defect, further work with this construct was not undertaken. Moreover, 16S rRNA derived from plasmids expressing untagged pre-16S rRNA or the pre-rRNA tagged at positions 105L, 11L and 20T was detected in 70S ribosomes at similar levels (Supplementary Fig. 1c and data not shown). These experiments also revealed no discernible change in ribosomal subunit distribution when pre-16S rRNA contains the MS2 tag or mature 16S rRNA was plasmid derived. The complementation analysis, lack of cold sensitivity and incorporation of tagged rRNA in mature ribosomes suggest that insertion of the tags at positions 105L, 11L and 20T does not affect ribosome biogenesis. These tagged pre-16S rRNA transcripts allowed affinity purification of pre-SSU RNPs from wild-type *E. coli* with less than 5% contamination with untagged rRNA (Supplementary Fig. 2). Thus, this system offers a robust and largely unperturbed means of isolating pre-SSU particles from exponentially growing *E. coli*.

17S rRNA is a predominant pre-16S rRNA species *in vivo*

Examination of pre-rRNA from the purified RNPs by denaturing gel electrophoresis (Fig. 2a), Northern blotting (Fig. 2b), modified 3′5′ RACE (Rapid amplification of cDNA ends) (Fig. 2c) and primer extension (data not shown) revealed that the predominant purified rRNA was 17S rRNA, the pre-SSU species liberated from the primary rRNA transcript by RNase III cleavage. Purification of assembly intermediates tagged at position 11L from an *E. coli* strain lacking RNase G, a 16S rRNA maturation enzyme, resulted in isolation of significant amounts of 16.3S rRNA (compared to the 17S rRNA) (Fig. 2d), consistent with previous results on pre-rRNA processing in this strain[12,22]. These data indicate that affinity purification can yield many pre-16S rRNA containing rRNPs and thus suggests that isolation of 17S rRNA from several tagged positions in wild-type *E. coli* is not due to other species being refractory to purification and suggest that 17S rRNA is a platform for assembly of pre-SSUs in the wild-type *E. coli*.

The 17S rRNA containing RNPs have distinct architecture

The conformation of 17S rRNA in the three purified RNPs was explored using chemical probing (kethoxal) and primer extension[25]. Each purified pre-SSU exhibited different rRNA

conformations, likely revealing different biogenesis snapshots occurring on the same 1690 nucleotide rRNA scaffold. We observed reactivity differences in both mature and leader regions of 17S rRNA (Fig. 3). Thus purification of architecturally diverse intermediates with the same length pre-rRNA could be due to availability of MS2 tags for MS2 coat protein binding as a result of distinct RNP conformations during biogenesis, *i.e.* the tags could be differentially available during pre-rRNA transcription, folding, processing and incremental protein binding. Notably, leader nucleotides exhibited different reactivity in the three intermediates (Fig. 3a); hence during biogenesis different conformations exist in intermediates. The reactivity of the MS2 tag nucleotides indicated that stem loop structure was properly formed, suggesting no significant interactions with the pre-rRNA molecule. Moreover, some of these changes are in agreement with prior work where the leader (from untagged 17S rRNA) interacts with mature 16S rRNA sequence[26,27] suggesting that tagged 17S rRNA can form these conformations and that tagging does not globally perturb rRNA conformation.

Additionally, many other conserved, functional nucleotides of mature 16S rRNA showed altered reactivity in the intermediates compared to mature SSUs, indicating that these 17S rRNA containing intermediates should be unable to enter the translational cycle (Fig. 3b, Supplementary Fig. 3). Some of the observed changes occur at nucleotides involved in pseudoknots[28,29,30] (nucleotides; 505, 506, 524, 527, 575, 917), tRNA interactions[31,32] (nucleotides; 530, 693, 926, 1401) and inter-subunit bridges[33–35] (nucleotides; 698, 700, 703, 705, 710, 711, 713, 760, 761, 763, 771, 776, 800, 894, 895, 898, 1415, 1416, 1419, 1421). In addition, there were many nucleotides that had similar reactivity between the intermediates; some of these had reactivity similar to mature SSUs [representative nucleotides; 143 – 211 (5′domain of 16S rRNA), 877 – 885 (central domain of 16S rRNA), 1220, 1221, 1222, 1278, 1279 (3′domain of 16S rRNA)]. These results suggest that there are some common folding pathways and that certain regions achieve “final” conformational states early in biogenesis (Supplementary Fig. 3). The probing data suggest that 20T tagged rRNPs most closely resembled mature SSUs while 105L tagged rRNPs were the most distinct from mature SSUs. Additionally, it was clear that the body of the pre-SSUs was more structurally similar to mature SSUs than the other domains in all three intermediates. These data reveal that the 17S rRNA containing RNPs are structurally distinct but all lack the formation of functional sites.

R-proteins are differentially associated with the pre-SSUs

To further investigate differences between the 17S rRNA containing RNPs, we examined r-protein association by label-free liquid chromatography-tandem mass spectrometry (LC-MS/MS) and spectral counting (Fig. 4, Supplementary Fig. 4). We used mature ribosomes, purified with an MS2 tag in the mature 16S rRNA (86M), as a normalization standard for r-protein association (Supplementary Data Set 2), allowing direct comparison of r-protein levels in intermediates to mature SSUs. No r-protein was found in any of the three 17S rRNA containing RNPs, at levels observed in mature SSUs (Fig. 4a, Supplementary Fig. 4a). R-protein, S4, which binds to the 5′ domain of 16S rRNA, corresponding to the SSU body, had approximately the same occupancy in all three intermediates. Three r-proteins, S2, S3 and S21 were highly underrepresented in all intermediates as compared to mature

SSUs (Fig. 4a, ≤38%). 105L tagged rRNPs had the lowest total r-protein association compared to the other two pre-SSUs and mature SSUs. 11L and 20T tagged rRNP had distinct r-protein association. Thus, distinct r-protein composition corroborates the different conformations observed in probing experiments and further supports that each affinity purified intermediate is distinct.

To further analyze the differential association of r-proteins to purified intermediates and examine whether r-proteins associate in groups to pre-SSUs, we calculated relative protein abundance (RPA, see Methods) and performed hierarchical clustering analysis (Fig. 4b, c, Supplementary Fig. 4b). This allowed calculation of relative protein association between intermediates (not relative to mature SSUs) in an unbiased, comprehensive manner, allowing r-protein binding to 17S rRNA to be studied in detail. We observed multiple pathways for r-protein association to the body and platform of 11L and 20T tagged rRNPs. R-proteins associating with the platform, S8 and S18 were relatively more abundant in 11L tagged RNPs as compared to 20T tagged rRNPs while S15 and S11 levels were elevated in 20T tagged RNPs when compared to 11L tagged pre-SSUs (Fig. 4b, c). In addition, this analysis revealed three r-protein groups (Fig. 4b, Supplementary Fig. 4c). Group 1 largely included r-proteins (r-protein S4 is an exception) enriched in 20T tagged pre-SSUs (including r-proteins S15 and S11). Group II represented the r-proteins that were more abundant in 11L tagged rRNPs (includes r-proteins, S8 and S18) as compared to the other two intermediates. Interestingly, 11L tagged pre-SSUs had increased r-protein S7 association (Group II) and several other r-proteins (Group III) that bind to the SSU head. This analysis reveals multiple pathways of r-protein association and domain assembly on 17S rRNA in wild-type *E. coli*. Although each intermediate had distinct r-protein association, the clustering analysis indicated that overall r-protein addition is in agreement with previous *in vitro* and *in vivo* work[36–38] (Supplementary Fig. 4c). Interestingly, late binding r-proteins S5 (Group III) and S12 (Group II), which play an important role in translational fidelity[39] and ribosome assembly[40,41], fall in two separate groups and were previously shown to assemble at similar rates[38,42]. However, S5 aids in the formation of the head region and was grouped with most r-proteins that bind the head (Fig. 4b) while S12 influences SSU body formation. The predominance of 17S rRNA, distinct architecture and r-protein complements in the *in vivo* formed intermediates suggest that 17S rRNA can be a major platform for SSU assembly in wild-type *E. coli*.

Independent 5′ and 3′ end maturation of 16S rRNA *in vivo*

Our results, and data from other groups, suggest multiple pathways for r-protein association and rRNA folding during SSU assembly *in vivo*[43,44]. However, whether further maturation of 17S rRNA to 16S rRNA also follows multiple or an obligatory pathway was not known. Modified 3′5′ RACE revealed a predominant 17S rRNA species purified using all three tags; however, minor, but detectable products of lengths between 17S rRNA and 16S rRNA were also observed (Fig. 2c). These minor products represented additional pre-16S rRNA maturation products (Fig. 5a, b), with either a mature 3′ end (in 105L and 11L tagged intermediates) or a mature 5′ end (in tag 20T intermediates). These data suggest that further maturation of 17S rRNA can be initiated at either the 5′ or 3′ end of 17S rRNA in wild-type *E. coli*. These results show that post-RNase III cleavage, 17S rRNA processing *in vivo* can

initiate at either end and like r-protein addition and rRNA folding, rRNA maturation can follow multiple pathways.

In vitro rRNA maturation of 17S rRNA containing RNPs

The authenticity of these 17S rRNA containing intermediates was further evaluated by incubation with wild-type extracts and examination of resulting rRNA species by modified 3′5′RACE (Fig. 5c), denaturing agarose gel and Northern analysis (data not shown). The 17S rRNA associated with the three different intermediates was processed into several shorter 16S rRNAs with maturation occurring at either or both the 5′ or 3′ end. The conversion of three different purified 17S rRNA complexes into primarily 16S rRNA suggests that these RNPs are capable of further maturation. The shorter pre-16S rRNA products observed during 17S rRNA maturation to 16S rRNA *in vitro* were consistent with those observed in purified intermediates *in vivo* (compare Fig. 5c with 5a, as depicted in Fig. 5b) suggesting 17S rRNA can undergo multiple maturation pathways *in vitro* and the purified rRNPs are most likely on-path SSU intermediates. Delayed rRNA processing, with accumulation of pre-16S rRNA, upon incubation of these intermediates with cell extracts lacking pre-16S rRNA processing enzymes, RNase G or RNase E[13], indicates that the processing of these purified 17S rRNA containing RNPs is defined (Supplementary Fig. 5). These data provide evidence that these purified RNPs are bona fide assembly intermediates in wild-type *E. coli*.

Discussion

An RNP affinity purification strategy was used to isolate *E. coli* SSU assembly intermediates formed in a wild-type strain. Our data revealed that 17S pre-rRNA acts as a major scaffold for SSU biogenesis in wild-type *E. coli*. 17S rRNA containing RNPs formed *in vivo* have distinct rRNA folding and r-protein association; these findings are consistent with the multiple SSU biogenesis pathways *in vivo*. Moreover, we observed additional rRNA maturation events at the 3′ or 5′ ends of 17S rRNA, both *in vivo* and *in vitro*, indicating that final end maturation can follow multiple pathways. Our results suggest that there are multiple pathways for SSU formation *in vivo* in wild-type *E. coli* for all aspects of biogenesis. We have established a system that allows examination of snapshots of RNP formation *in vivo* and characterization of various biogenesis processes.

A requirement for processing and maturation of cellular RNAs is common throughout all kingdoms of life. Initial processing of double stranded precursor RNAs is conserved for many cellular RNAs including microRNAs and rRNAs[8,12,45]. For bacterial rRNAs, RNase III, a double stranded RNA endonuclease, likely acts early in biogenesis once transcription of pre-16S rRNA is completed and RNase III cleavage sites become available (see Fig. 1a); longer pre-rRNA transcripts, uncut by RNase III, are rarely detected *in vivo*[10,11]. Our data, suggesting that this RNase III cleavage product, 17S rRNA, is a platform for biogenesis and these data are consistent with results from mutant bacterial strains where 17S rRNA accumulation is observed upon disruption of most genes associated with SSU biogenesis[17,18]. Our data in wild-type *E. coli* along with previous data indicates that 17S rRNA is the major platform for SSU biogenesis.

Maturation of 17S rRNA and stable association of a full complement of r-proteins are likely rate limiting during SSU biogenesis. In a primary transcript, a double stranded helix formed by the leader and trailer is required for RNase III cleavage (17S rRNA production). Helical elements might persist in 17S rRNA and could be inhibitory to further 17S rRNA maturation[12]. Our data suggest that the leader can adopt different conformations at various stages of biogenesis (Fig 3a). Mutations or deletions in the leader affect SSU formation[27,46,47] and the leader can interact with mature 16S rRNA sequences at different stages of biogenesis[48]. Moreover, cryo-electron microscopy studies have failed to detect densities for unprocessed sequences[49–51] further suggesting that it might be a flexible and multi-structured during biogenesis and explains why there is no defined structure for pre-rRNA elements unlike mature 16S rRNA. The different conformations of pre-rRNA could influence the solvent accessibility of MS2 tag present in this region, thus allowing us to purify distinct intermediates with differently positioned tags.

Several lines of evidence suggest that the affinity purified pre-rRNPs are on-path. First, insertion of tags in precursor regions of 16S rRNA do not perturb ribosome biogenesis as these rDNA constructs were able to complement growth at wild-type untagged levels as a sole source of rDNA[24] and did not exhibit cold-sensitivity. Additionally, rRNA from rDNA plasmids containing tags in precursor regions were incorporated into 70S ribosomes at similar levels as untagged plasmid-derived rRNA (Fig. 1c, Supplementary Fig. 1). Moreover, these 17S rRNAs can be converted into 16S rRNA *in vitro* (Fig. 5). This maturation follows multiple pathways and is dependent on pre-16S rRNA processing enzymes (Supplementary Fig. 5). 17S rRNA containing pre-SSU intermediates in single deletion strains Δ*rsgA*[49], Δ*rimM*[50–52] and Δ*rbfA*[52] and double deletion strain Δ*rbfA*Δ*rsgA*[51] showed several snapshots of SSU assembly with differential levels of r-proteins association and distinct architectures suggesting multiple pathways of SSU formation. Our chemical probing and r-protein addition data are consistent with the changes observed in intermediates accumulated in these deletion strains. However, our work offers the first analysis in wild-type *E. coli* growing at 37°C affording a detailed dissection of SSU biogenesis *in vivo*.

Chemical probing with kethoxal showed varying degrees of susceptibility of nucleotides to modification (Fig. 3, Supplementary Fig. 3). One possibility is that each intermediate is composed of a consortium of heterogeneous but related intermediates that yield differential levels of reactivity. Another possibility is that conformational changes occur at different stages, yet ultimately achieve a functional structure. This later possibility is supported by differential r-protein association to 17S rRNA *in vivo* (Fig. 4, Supplementary Fig. 4). In addition, strong thermodynamic dependencies observed *in vitro* and illustrated in the SSU assembly map do not always hold true *in vivo* (see Supplementary Fig. 4c). Several r-proteins (S6, S9, S13, S15, S17 and S20) are non-essential *in vivo*[53] whereas they are indispensable for *in vitro* reconstitution[54,55]. R-protein, S15 is essential for assembly of the platform *in vitro* but the gene encoding S15 (*rpsO*) can be deleted *in vivo* and SSUs can still appropriately assemble the platform[56]. Additionally, contrary to predictions from *in vitro* data, the 5′ domain of 16S rRNA can fold correctly in the absence of r-proteins S17 and S20 (ref. 57). The kinetic analysis of r-protein addition *in vitro* as well as *in vivo*[38,43] and

concurrent binding of r-proteins to several regions of 16S rRNA during *in vitro* assembly further suggest the existence of multiple assembly pathways[44]. We cannot rule out the possibility that some r-proteins are weakly bound in the intermediates and may dissociate during purification. This would suggest that these r-proteins exhibit stability differences among intermediates, which are consistent with induced-fit and multi-phasic SSU assembly[44]. While it has been shown that r-proteins have complex kinetics and that parallel pathways exist, it was unclear if these parallel pathways were dependent on different pre-rRNA scaffolds or if these pathways were obligate depending on the pre-rRNA to which they bind during the cascade. Our analysis suggests that 17S rRNA is a major pre-16S rRNA species for these multiple pathways.

We have established that intermediates have distinct conformations and r-protein association but the general functional regions in the intermediates are not in mature conformations. Sites involved in the process of translation showed altered conformation in isolated intermediates suggesting that 17S rRNA containing rRNPs are not fully functional (Fig. 3b). The non-functional state of pre-rRNPs is supported by r-protein data: two translation-important r-proteins (S5 and S12) are differentially associated with the distinct pre-rRNPs, suggesting that while distinct pathways are followed there are similarities in the overall capacity of SSU intermediates. As bacteria lacks nuclear compartmentalization, the retention of the spacer sequences may aid in sequestration of immature SSUs from the translational cycle and act in SSU quality control, which occurs in the nucleolus in eukaryotes. A U3 boxA-like sequence in the leader has been proposed to act as a chaperone for central pseudoknot formation[58]. Specific conditions that allow 17S rRNA or intermediate pre-16S rRNA to be incorporated into 70S-like ribosomes, which has detrimental effects on translation[19,27]. Thus, the presence of 17S rRNA in RNPs with “immature” functional sites in wild-type bacteria suggests a mechanism that allows maturation and function of SSUs in the same cellular environment without deleterious consequences.

While there are many obvious differences between these purified intermediates, there are also commonalities between them. The length of the purified pre-rRNA is the most obvious, 17S rRNA (Fig. 2a). Our chemical probing data suggests that the SSU body (5′ domain of 16S rRNA), is most similar between all intermediates and mature SSUs (Fig. 3b). A common theme was revealed where most functional sites are not formed in any of these pre-SSUs. Moreover, r-protein S4 is equally represented in all three intermediates and S4 is generally regarded as an early binding protein[36,55]. In contrast, r-proteins S2, S3 and S21, which have all been shown to bind late and with slow kinetics[38,55,59] are depleted in these intermediates. The relative lack of r-protein S21 is of particular note as it is important for proper translational initiation[19,60]. Therefore, while it appears that there are multiple pathways for SSU formation *in vivo*, a common theme to limit functional site formation until later in biogenesis and thus likely preclude immature subunits from entering the translational cycle has emerged.

Our data indicates that ribosome biogenesis occurs via multiple pathways *in vivo*. Multiple *in vivo* pathways for r-protein addition and 17S rRNA maturation in wild-type *E. coli* can be observed (see Fig. 5, Supplementary Fig. 5). Additionally, there are multiple pathways for auxiliary factor action on 17S rRNA containing RNPs *in vivo* (N.G., G.M.C., unpublished

results). Thus several SSU biogenesis processes occur simultaneously in multiple pathways on 17S rRNPs to ultimately form mature, functional subunits. This work highlights the potential of *E. coli* to adapt under different circumstances and challenges in antimicrobial development. This is the first work that allows concurrent analysis of rRNA processing, r-protein binding and rRNA conformational changes, yielding comprehensive analysis of SSU intermediates and assembly pathways. This work is a major advance in our understanding of *in vivo* formation of ribosomal subunits. Perhaps as importantly, this system provides the potential to study most other dynamic functional RNPs *in vivo*.

Methods

Insertion of MS2 tags in transcribed spacers of 16S rRNA

pLK35 plasmid containing an rDNA operon under the control of lambda P_L promoter and ampicillin resistance marker was used for MS2 tag insertion[61]. A selectable marker C1192U (spectinomycin resistance[62,63]) in 16S rRNA was introduced by site-directed mutagenesis (Quikchange XL, Stratagene). The spacer sequences of 16S rRNA (leader and trailer) from all seven rDNA operons of *E. coli* were aligned using ClustalW 2.0 (ref. 64). The variant nucleotides at position 21 in trailer and 11 in leader along with additional non-variant positions in leader were chosen for MS2 tag insertion (Nucleotide numbering same as in Fig. 1a). MS2 tags were placed between nucleotides 105 and 106 (105L), nucleotides 86 and 87 (86L), 11 and 12 (11L) in the leader and 20 and 21 (20T) in the trailer using protocols described previously[21]. The insertion of MS2 tag was confirmed by sequencing by GENEWIZ (South Plainfield, NJ). The plasmid referred to as pSpurMS2(ref. 21) with MS2 tag in mature 16S rRNA was renamed as 86M.

Growth analysis of rDNA plasmids containing MS2 tags

Plasmids containing the MS2 tag and a non-tagged plasmid were transformed and shuffled in a Δ7*rrn* strain, MC338, lacking chromosomal rDNA operons and carrying a wild-type rDNA on a plasmid, pCsacB7(ref. 24,65). LB media containing ampicillin (100μg/ml) was inoculated with overnight saturated cultures at an optical density of 0.01 at 600 nm (OD_{600}) and cells were then grown at 37°C. The growth supported by the tagged ribosomes in the absence of wild-type ribosomes was monitored by measuring OD_{600}. The experiment was done in triplicates and the average OD_{600} was plotted on a semi-log scale. The difference in growth rate among the strains with different tagged plasmids was calculated during the exponential phase of growth.

Plasmids containing MS2 tagged rDNA operons and pLK35 were transformed in *E. coli* strain MRE600 (carrying all seven chromosomal rDNA operons). Growth of these strains was monitored and analyzed at 25°C as described above.

Expression and purification of MS2 fusion coat protein

The two mutations, V75E and A81G, were introduced in the MS2 coat protein of MBP–MS2–6X His fusion protein in pMAL–c2g vector to prevent oligomerization[66] by site-directed mutagenesis (Quikchange XL, Stratagene). Mutations were confirmed by sequencing (GENEWIZ).

BL21(DE3) carrying pMBP–MS2(V75E,A81G)–6X His were grown at 37°C in Terrific Broth media with ampicillin (100μg/ml) until OD_{600} of 0.6, overexpression of the fusion protein was induced by 1mM IPTG (isopropyl-beta-D-thiogalactopyranoside) and were grown further for 3 hours. Cells were pelleted and resuspended in lysis buffer (20mM Na_2PO_4 [pH=7.0], 500mM NaCl, 10mM Imidazole) and lysed using a high pressure homogenizer (Avestin Emulsiflex C3). Lysate was incubated with 1/100U per culture volume of Amplification grade DNase I (Sigma Aldrich) for 10 minutes on ice. The clarified lysate was loaded on a HiTrap Chelating column equilibrated with 0.1M Nickel sulfate using Fast Performance Liquid Chromatography (GE Healthcare AKTA). The protein was eluted with elution buffer (20mM Na_2PO_4 [pH =7.0], 500mM NaCl, 500mM imidazole) according to the manufacture's protocol. The purified MS2 fusion protein was dialyzed overnight in storage buffer (80mM HEPES [pH=7.4], 1M KCl, 10mM $MgCl_2$, 10% Glycerol), diluted to a concentration of 1mg/ml and stored at –80°C.

Purification of the SSU intermediates

MRE600, carrying plasmids with MS2 tagged rDNA operon, were grown at 37°C in LB media with ampicillin (100 μg/ml) and 0.2% glucose until OD_{600} reached 0.6. Cells were cooled, pelleted, resuspended in MBP binding buffer (20mM Tris-HCl [pH=7.4], 100mM KCl, 10mM $MgCl_2$, 1mM EDTA) and lysed using a high pressure homogenizer. 1/100U of amplification grade DNase I was added to the lysate and incubated on ice for 10 minutes. The clarified lysate was incubated with amylose beads (New England Biolabs) which were pre-bound with MS2 fusion protein, for 2 hours on a rotating platform at 4°C. The beads were washed with 40 bead volumes of binding buffer, 20 bead volumes of washing buffer (20mM Tris-HCl [pH=7.4], 200mM KCl, 10mM $MgCl_2$, 1mM EDTA) and then packed into a column. The beads were washed again with a 15 column volume of washing buffer. The tagged assembly intermediates were isolated with elution buffer (20mM Tris-HCl [pH=7.4], 500mM KCl, 10mM $MgCl_2$, 1mM EDTA). Allele specific primer extension for the C1192U change in plasmid borne 16S rRNA was performed to check the purity of the isolated intermediates as described previously[28,67].

RNA isolation and analysis

The RNA was isolated from the purified MS2 tagged RNPs as described[25]. 1μg of the RNA isolated from each elution fraction of the purified rRNA containing assembly intermediates was resolved on formaldehyde containing 2% denaturing agarose gel. The gel was visualized using a BioRad Versa Doc. Northern analysis was performed as described with the following oligos[19]: mature 16S – 5′-CGCATTTCACCGCTACA-3′, leader – 5′-CGTGTTCACTCTTGAGACTTGG-3′ and trailer 5′-CAAAGTACGCTTCTTTAAG-3′

Modified 3′5′ RACE was performed as outlined with the following modifications[68]. 200ng of purified RNA was used for initial circularization with T4 RNA ligase (New England Biolabs) overnight at 16°C. This step was done with and without a heat denaturation step. For heat denaturation, RNA was heated at 74°C and cooled quickly before ligation. Reverse transcription was performed with AMV reverse transcriptase (New England Biolabs) for 60 minutes followed by PCR amplification. The PCR amplified products were resolved on a 2% agarose gel and visualized using the Bio-Rad Versa Doc system. To sequence the

different 3′5′ RACE products, the products were gel purified with Illustra GFX PCR DNA and Gel Band Purification kit (GE Healthcare) and PCR amplified using the same primers as for initial PCR reaction. The PCR products were resolved on a 2% agarose gel to check the purity and re-purified as described above. The purified products were sequenced by GENEWIZ.

Chemical probing

Chemical probing by kethoxal was performed as detailed[25,69]. The purified rRNA containing RNPs were concentrated using Spin-X UF 500, MWCO 5000 (Corning) and buffer exchanged in RA^+ buffer (80mM HEPES [pH = 7.6], 20mM $MgCl_2$, 330mM KCl, 0.01% Nikkol). 25 μg of mature small subunits, naked 16S rRNA and purified tagged RNPs were incubated with 0.4% kethoxal on ice for 60 minutes. Primer extensions were performed and the products were resolved on a 6% sequencing urea-polyacrylamide gel to visualize the modifications[70]. The intensity of nucleotide modifications in the mature 16S rRNA region was quantified using SAFA[71] and ImageJ[72]. The change in nucleotide intensity of purified intermediates (I_I) and naked 16S rRNA (I_N) was compared with mature small subunits (I_M). Nucleotides showing consistent changes in at least two experiments were averaged. The relative change (RC) in reactivity was calculated as RC= $\log_2$ (I_I/ I_M) or RC= $\log_2$ (I_N/ I_M) and plotted as a histogram (Supplementary Fig.3, Supplementary Data Set 1). Only values of $-0.55 < RC > 0.55$ (or change in reactivity of greater than 50% as compared to mature SSU) for nucleotide reactivity change were considered as protected or exposed. For plotting these changes on the 3D structure, changes in the nucleotide reactivity were binned as follow: $0.55<|RC|\leq 1$ were considered as a weak enhancement or protection and represented by small circles while $|RC|>1$ was considered as a strong enhancement or protection, represented by large circles. The changes were plotted on the 3D structure of SSU showing only 16S rRNA (PDB: 2AVY). The nucleotide reactivity changes in the leader were measured with ImageJ[72] and plotted as weak (small circles) and strong (large circles) changes.

Ribosomal protein analysis

The purified RNPs were concentrated and buffer exchanged into 6M Urea, 10mM DTT solution as described above. They were normalized to equal RNA concentration by measuring OD_{260} with Nanodrop (Thermo Scientific). All quantitative results were obtained from three biological replicates and two technical replicates performed for each sample. LC-MS/MS analysis was performed by the URMC Proteomics Center at University of Rochester. The protein search was done with Mascot software (Matrix Science Inc) and spectral counts were calculated with ProteoIQ (Premier Biosoft). The spectral count of each protein in a sample was normalized according to the total spectral count of the sample. The spectral counts were averaged for each protein in biological and technical replicates in each intermediate and 86M to improve protein quantification (Supplementary Data Set 2). Relative levels of r-proteins associated with the intermediates were compared to those associated with 86M and the ratios were expressed as percentages. The relative levels were binned into three groups and plotted on the 3D structure of SSU as a heat map (Fig. 4a, Supplementary Fig 4a). To calculate Relative Protein Abundance (RPA) for individual r-protein present in three intermediates, the relative levels of each r-protein (ratio of intermediate and mature SSU) among the three intermediates were median centered and $\log_2$

transformed and followed by hierarchical clustering analysis by Cluster3.0(ref. 73) and visualized using Java TreeView[74].

In vitro processing analysis

The purified intermediates were concentrated and buffer exchanged (20mM Tris-HCl [pH7.4], 100mM KCl, 10mM $MgCl_2$, 1mM EDTA, and 6mM BME). S100 extracts[75] were prepared from MRE600 strain (wild-type) along with Δ*rng* and *rne*^{ts} strains of *E. coli*[13,14]. Purified intermediates were incubated with different S100 extracts (containing 100 μM ATP and GTP) at 37°C. Aliquots were taken at 0 and 60 minutes time points and the length and identity of pre-16S RNA were analyzed by the methods described above.

Ribosome sedimentation profile analysis

Wild-type strain carrying non-tagged and tagged plasmids were grown to OD_{600} of 0.5 at 37°C. The ribosome profiles were obtained as described previously[76]. Various fractions were collected and ethanol precipitated for RNA extraction and analysis by allele specific primer extension as described above. Percentages of plasmid-borne rRNA were calculated using ImageJ software as described above.

Supplementary Material

Refer to Web version on PubMed Central for supplementary material.

Acknowledgements

We thank D. Ermolenko and E. Phizicky for critical discussions during the preparation of the manuscript as well as the members of Culver Lab for helpful discussions and technical advice. We thank F. Hagen and University of Rochester Proteomics Facility for mass spectrometry analysis. We thank G. Salahura for technical assistance. We thank R. Green (Johns Hopkins University) for 86M (Spur) and MS2 coat protein overexpression constructs and M. O'Connor (University of Missouri-Kansas City) for MC338 strain. This work was supported by US National Institute of Health grant GM62432 to G.M.C.

References

1. Kaczanowska M, Ryden-Aulin M. Ribosome biogenesis and the translation process in *Escherichia coli*. Microbiol Mol Biol Rev. 2007; 71:477–494. [PubMed: 17804668]
2. Kressler D, Hurt E, Bassler J. Driving ribosome assembly. Biochim Biophys Acta. 2010; 1803:673–683. [PubMed: 19879902]
3. Borg S, et al. Novel *Salmonella typhimurium* properties in host-parasite interactions. Immunol Lett. 1999; 68:247–249. [PubMed: 10424427]
4. Bjorkman J, Samuelsson P, Andersson DI, Hughes D. Novel ribosomal mutations affecting translational accuracy, antibiotic resistance and virulence of *Salmonella typhimurium*. Mol Microbiol. 1999; 31:53–58. [PubMed: 9987109]
5. Phunpruch S, et al. A role for 16S rRNA dimethyltransferase (ksgA) in intrinsic clarithromycin resistance in *Mycobacterium tuberculosis*. Int J Antimicrob Agents. 2013; 41:548–551. [PubMed: 23541074]
6. Ilina EN, et al. Mutation in ribosomal protein S5 leads to spectinomycin resistance in *Neisseria gonorrhoeae*. Front Microbiol. 2013; 4:186. [PubMed: 23847609]
7. Champney WS. The other target for ribosomal antibiotics: inhibition of bacterial ribosomal subunit formation. Infect Disord Drug Targets. 2006; 6:377–390. [PubMed: 17168803]

8. Falaleeva M, Stamm S. Processing of snoRNAs as a new source of regulatory non-coding RNAs: snoRNA fragments form a new class of functional RNAs. Bioessays. 2013; 35:46–54. [PubMed: 23180440]
9. Srivastava AK, Schlessinger D. Mechanism and regulation of bacterial ribosomal RNA processing. Annu Rev Microbiol. 1990; 44:105–129. [PubMed: 1701293]
10. Kindler P, Keil TU, Hofschneider PH. Isolation and characterization of a ribonuclease III deficient mutant of *Escherichia coli*. Mol Gen Genet. 1973; 126:53–59. [PubMed: 4591369]
11. Young RA, Steitz JA. Complementary sequences 1700 nucleotides apart form a ribonuclease III cleavage site in *Escherichia coli* ribosomal precursor RNA. Proc Natl Acad Sci U S A. 1978; 75:3593–3597. [PubMed: 358189]
12. Deutscher MP. Maturation and degradation of ribosomal RNA in bacteria. Prog Mol Biol Transl Sci. 2009; 85:369–391. [PubMed: 19215777]
13. Li Z, Pandit S, Deutscher MP. RNase G (CafA protein) and RNase E are both required for the 5' maturation of 16S ribosomal RNA. EMBO J. 1999; 18:2878–2885. [PubMed: 10329633]
14. Wachi M, Umitsuki G, Shimizu M, Takada A, Nagai K. *Escherichia coli cafA* gene encodes a novel RNase, designated as RNase G, involved in processing of the 5' end of 16S rRNA. Biochem Biophys Res Commun. 1999; 259:483–488. [PubMed: 10362534]
15. Sulthana S, Deutscher MP. Multiple exoribonucleases catalyze maturation of the 3' terminus of 16S ribosomal RNA (rRNA). J Biol Chem. 2013; 288:12574–12579. [PubMed: 23532845]
16. Jacob AI, Kohrer C, Davies BW, RajBhandary UL, Walker GC. Conserved bacterial RNase YbeY plays key roles in 70S ribosome quality control and 16S rRNA maturation. Mol Cell. 2013; 49:427–438. [PubMed: 23273979]
17. Connolly K, Culver G. Deconstructing ribosome construction. Trends Biochem Sci. 2009; 34:256–263. [PubMed: 19376708]
18. Shajani Z, Sykes MT, Williamson JR. Assembly of bacterial ribosomes. Annu Rev Biochem. 2011; 80:501–526. [PubMed: 21529161]
19. Connolly K, Culver G. Overexpression of RbfA in the absence of the KsgA checkpoint results in impaired translation initiation. Mol Microbiol. 2013; 87:968–981. [PubMed: 23387871]
20. Lindahl L. Intermediates and time kinetics of the *in vivo* assembly of *Escherichia coli* ribosomes. J Mol Biol. 1975; 92:15–37. [PubMed: 1097701]
21. Youngman EM, Green R. Affinity purification of *in vivo*-assembled ribosomes for *in vitro* biochemical analysis. Methods. 2005; 36:305–312. [PubMed: 16076457]
22. Youngman EM, Brunelle JL, Kochaniak AB, Green R. The active site of the ribosome is composed of two layers of conserved nucleotides with distinct roles in peptide bond formation and peptide release. Cell. 2004; 117:589–599. [PubMed: 15163407]
23. Persaud C, et al. Mutagenesis of the modified bases, m(5)U1939 and psi2504, in *Escherichia coli* 23S rRNA. Biochem Biophys Res Commun. 2010; 392:223–227. [PubMed: 20067766]
24. Asai T, et al. Construction and initial characterization of *Escherichia coli* strains with few or no intact chromosomal rRNA operons. J Bacteriol. 1999; 181:3803–3809. [PubMed: 10368156]
25. Moazed D, Stern S, Noller HF. Rapid chemical probing of conformation in 16S ribosomal RNA and 30S ribosomal subunits using primer extension. J Mol Biol. 1986; 187:399–416. [PubMed: 2422386]
26. Dammel CS, Noller HF. A cold-sensitive mutation in 16S rRNA provides evidence for helical switching in ribosome assembly. Genes Dev. 1993; 7:660–670. [PubMed: 7681419]
27. Roy-Chaudhuri B, Kirthi N, Culver GM. Appropriate maturation and folding of 16S rRNA during 30S subunit biogenesis are critical for translational fidelity. Proc Natl Acad Sci U S A. 2010; 107:4567–4572. [PubMed: 20176963]
28. Powers T, Noller HF. A functional pseudoknot in 16S ribosomal RNA. EMBO J. 1991; 10:2203–2214. [PubMed: 1712293]
29. Vila A, Viril-Farley J, Tapprich WE. Pseudoknot in the central domain of small subunit ribosomal RNA is essential for translation. Proc Natl Acad Sci U S A. 1994; 91:11148–11152. [PubMed: 7526390]

30. Poot RA, van den Worm SH, Pleij CW, van Duin J. Base complementarity in helix 2 of the central pseudoknot in 16S rRNA is essential for ribosome functioning. Nucleic Acids Res. 1998; 26:549–553. [PubMed: 9421514]
31. Moazed D, Noller HF. Binding of tRNA to the ribosomal A and P sites protects two distinct sets of nucleotides in 16S rRNA. J Mol Biol. 1990; 211:135–145. [PubMed: 2405162]
32. Yusupova GZ, Yusupov MM, Cate JH, Noller HF. The path of messenger RNA through the ribosome. Cell. 2001; 106:233–241. [PubMed: 11511350]
33. Noller HF, et al. Structure of the ribosome at 5.5Å resolution and its interactions with functional ligands. Cold Spring Harb Symp Quant Biol. 2001; 66:57–66. [PubMed: 12762008]
34. Schuwirth BS, et al. Structures of the bacterial ribosome at 3.5Å resolution. Science. 2005; 310:827–834. [PubMed: 16272117]
35. Nguyenle T, Laurberg M, Brenowitz M, Noller HF. Following the dynamics of changes in solvent accessibility of 16S and 23S rRNA during ribosomal subunit association using synchrotron-generated hydroxyl radicals. J Mol Biol. 2006; 359:1235–1248. [PubMed: 16725154]
36. Culver GM. Assembly of the 30S ribosomal subunit. Biopolymers. 2003; 68:234–249. [PubMed: 12548626]
37. Chen SS, Sperling E, Silverman JM, Davis JH, Williamson JR. Measuring the dynamics of *E. coli* ribosome biogenesis using pulse-labeling and quantitative mass spectrometry. Mol Biosyst. 2012; 8:3325–3334. [PubMed: 23090316]
38. Mulder AM, et al. Visualizing ribosome biogenesis: parallel assembly pathways for the 30S subunit. Science. 2010; 330:673–677. [PubMed: 21030658]
39. Ogle JM, Carter AP, Ramakrishnan V. Insights into the decoding mechanism from recent ribosome structures. Trends Biochem Sci. 2003; 28:259–266. [PubMed: 12765838]
40. Kirthi N, Roy-Chaudhuri B, Kelley T, Culver GM. A novel single amino acid change in small subunit ribosomal protein S5 has profound effects on translational fidelity. RNA. 2006; 12:2080–2091. [PubMed: 17053085]
41. Calidas D, Lyon H, Culver GM. The N-terminal extension of S12 influences small ribosomal subunit assembly in *Escherichia coli*. RNA. 2014; 20:321–330. [PubMed: 24442609]
42. Held WA, Mizushima S, Nomura M. Reconstitution of *Escherichia coli* 30S ribosomal subunits from purified molecular components. J Biol Chem. 1973; 248:5720–5730. [PubMed: 4579428]
43. Chen SS, Williamson JR. Characterization of the ribosome biogenesis landscape in *E. coli* using quantitative mass spectrometry. J Mol Biol. 2013; 425:767–779. [PubMed: 23228329]
44. Adilakshmi T, Bellur DL, Woodson SA. Concurrent nucleation of 16S folding and induced fit in 30S ribosome assembly. Nature. 2008; 455:1268–1272. [PubMed: 18784650]
45. Yates LA, Norbury CJ, Gilbert RJ. The long and short of microRNA. Cell. 2013; 153:516–519. [PubMed: 23622238]
46. Mori H, Dammel C, Becker E, Triman K, Noller HF. Single base alterations upstream of the *E. coli* 16S rRNA coding region result in temperature-sensitive 16S rRNA expression. Biochim Biophys Acta. 1990; 1050:323–327. [PubMed: 2145040]
47. Balzer M, Wagner R. Mutations in the leader region of ribosomal RNA operons cause structurally defective 30S ribosomes as revealed by *in vivo* structural probing. J Mol Biol. 1998; 276:547–557. [PubMed: 9551096]
48. Besancon W, Wagner R. Characterization of transient RNA-RNA interactions important for the facilitated structure formation of bacterial ribosomal 16S RNA. Nucleic Acids Res. 1999; 27:4353–4362. [PubMed: 10536142]
49. Jomaa A, et al. Understanding ribosome assembly: the structure of *in vivo* assembled immature 30S subunits revealed by cryo-electron microscopy. RNA. 2011; 17:697–709. [PubMed: 21303937]
50. Leong V, Kent M, Jomaa A, Ortega J. *Escherichia coli rimM* and *yjeQ* null strains accumulate immature 30S subunits of similar structure and protein complement. RNA. 2013; 19:789–802. [PubMed: 23611982]
51. Guo Q, et al. Dissecting the *in vivo* assembly of the 30S ribosomal subunit reveals the role of RimM and general features of the assembly process. Nucleic Acids Res. 2013; 41:2609–2620. [PubMed: 23293003]

52. Clatterbuck Soper SF, Dator RP, Limbach PA, Woodson SA. *In Vivo* X-Ray Footprinting of Pre-30S Ribosomes Reveals Chaperone-Dependent Remodeling of Late Assembly Intermediates. Mol Cell. 2013; 52:506–516. [PubMed: 24207057]
53. Bubunenko M, Baker T, Court DL. Essentiality of ribosomal and transcription antitermination proteins analyzed by systematic gene replacement in *Escherichia coli*. J Bacteriol. 2007; 189:2844–2853. [PubMed: 17277072]
54. Mizushima S, Nomura M. Assembly mapping of 30S ribosomal proteins from *E. coli*. Nature. 1970; 226:1214. [PubMed: 4912319]
55. Held WA, Ballou B, Mizushima S, Nomura M. Assembly mapping of 30S ribosomal proteins from *Escherichia coli*. Further studies. J Biol Chem. 1974; 249:3103–3111. [PubMed: 4598121]
56. Bubunenko M, et al. 30S ribosomal subunits can be assembled *in vivo* without primary binding ribosomal protein S15. RNA. 2006; 12:1229–1239. [PubMed: 16682557]
57. Adilakshmi T, Ramaswamy P, Woodson SA. Protein-independent folding pathway of the 16S rRNA 5' domain. J Mol Biol. 2005; 351:508–519. [PubMed: 16023137]
58. Dennis PP, Russell AG, Moniz De Sa M. Formation of the 5' end pseudoknot in small subunit ribosomal RNA: involvement of U3-like sequences. RNA. 1997; 3:337–343. [PubMed: 9085841]
59. Talkington MW, Siuzdak G, Williamson JR. An assembly landscape for the 30S ribosomal subunit. Nature. 2005; 438:628–632. [PubMed: 16319883]
60. Van Duin J, Wijnands R. The function of ribosomal protein S21 in protein synthesis. Eur J Biochem. 1981; 118:615–619. [PubMed: 7028483]

References for Methods Section

61. Douthwaite S, Powers T, Lee JY, Noller HF. Defining the structural requirements for a helix in 23S ribosomal RNA that confers erythromycin resistance. J Mol Biol. 1989; 209:655–665. [PubMed: 2685326]
62. Sigmund CD, Ettayebi M, Morgan EA. Antibiotic resistance mutations in 16S and 23S ribosomal RNA genes of *Escherichia coli*. Nucleic Acids Res. 1984; 12:4653–4663. [PubMed: 6330677]
63. Makosky PC, Dahlberg AE. Spectinomycin resistance at site 1192 in 16S ribosomal RNA of *E. coli*: an analysis of three mutants. Biochimie. 1987; 69:885–889. [PubMed: 2447957]
64. Larkin MA, et al. Clustal W and Clustal X version 2.0. Bioinformatics. 2007; 23:2947–2948. [PubMed: 17846036]
65. Sun Q, Vila-Sanjurjo A, O'Connor M. Mutations in the intersubunit bridge regions of 16S rRNA affect decoding and subunit-subunit interactions on the 70S ribosome. Nucleic Acids Res. 2011; 39:3321–3330. [PubMed: 21138965]
66. LeCuyer KA, Behlen LS, Uhlenbeck OC. Mutants of the bacteriophage MS2 coat protein that alter its cooperative binding to RNA. Biochemistry. 1995; 34:10600–10606. [PubMed: 7544616]
67. Xu Z, Culver GM. Differential assembly of 16S rRNA domains during 30S subunit formation. RNA. 2010; 16:1990–2001. [PubMed: 20736336]
68. Al Refaii A, Alix JH. Ribosome biogenesis is temperature-dependent and delayed in *Escherichia coli* lacking the chaperones DnaK or DnaJ. Mol Microbiol. 2009; 71:748–762. [PubMed: 19054328]
69. Xu Z, Culver GM. Chemical probing of RNA and RNA/protein complexes. Methods Enzymol. 2009; 468:147–165. [PubMed: 20946769]
70. Stern S, Moazed D, Noller HF. Structural analysis of RNA using chemical and enzymatic probing monitored by primer extension. Methods Enzymol. 1988; 164:481–489. [PubMed: 2468070]
71. Das R, Laederach A, Pearlman SM, Herschlag D, Altman RB. SAFA: semi-automated footprinting analysis software for high-throughput quantification of nucleic acid footprinting experiments. RNA. 2005; 11:344–354. [PubMed: 15701734]
72. Schneider CA, Rasband WS, Eliceiri KW. NIH Image to ImageJ: 25 years of image analysis. Nat Methods. 2012; 9:671–675. [PubMed: 22930834]
73. Eisen MB, Spellman PT, Brown PO, Botstein D. Cluster analysis and display of genome-wide expression patterns. Proc Natl Acad Sci U S A. 1998; 95:14863–14868. [PubMed: 9843981]

74. Saldanha AJ. Java Treeview-extensible visualization of microarray data. Bioinformatics. 2004; 20:3246–3248. [PubMed: 15180930]

75. Maki JA, Schnobrich DJ, Culver GM. The DnaK chaperone system facilitates 30S ribosomal subunit assembly. Mol Cell. 2002; 10:129–138. [PubMed: 12150913]

76. Connolly K, Rife JP, Culver G. Mechanistic insight into the ribosome biogenesis functions of the ancient protein KsgA. Mol Microbiol. 2008; 70:1062–1075. [PubMed: 18990185]

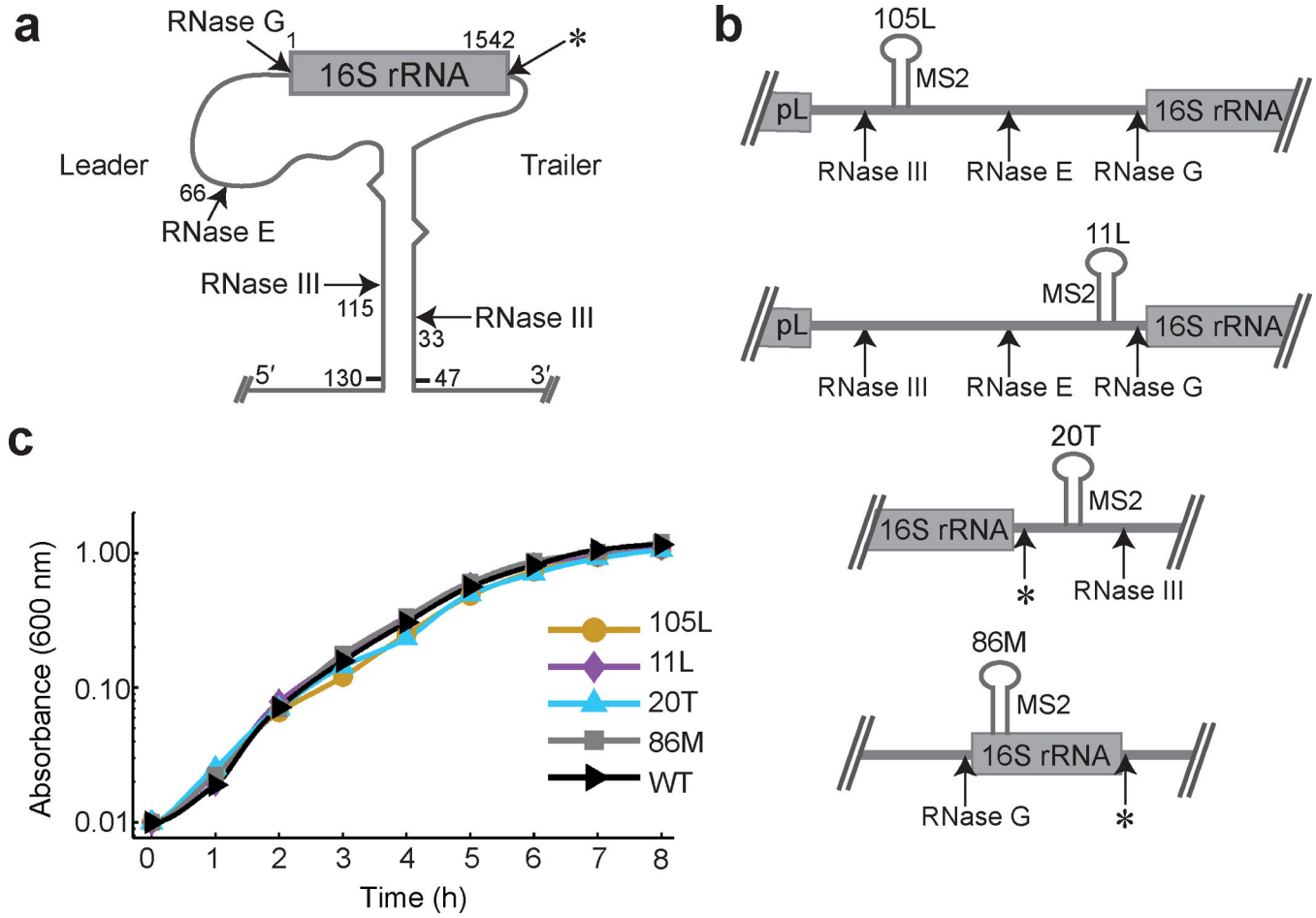

Figure 1. Affinity Purification of SSU intermediates

(**a**) Schematic of 16S rRNA maturation. Precursor 16S rRNA is cleaved by several RNases to form mature 16S rRNA. Cleavage sites and RNases involved are as indicated. * indicate PNPase, RNase PH, RNase R, RNase II and YbeY, the RNases implicated in 3′end maturation of 16S rRNA[13–16]. During transcription, leader and trailer base pairs to form double helicalstructure encompassing entire 16S rRNA and the helix contains the site for RNase III cleavage. The numbers represent the nucleotides away from the mature ends. (**b**) Sites of MS2 tag (marked as MS2) insertion for tag 105L, 11L, 20T and 86M. Tag 105L is 105nts (nucleotides) into the Leader and between the RNase III and RNase E cleavage sites. Tag 11L is 11nts into the Leader and placed between RNase E and RNase G cleavage sites. 20T tag is 20nts into the Trailer. Tag 86M is 86nts into the Mature 16S rRNA and has been previously used to isolate mature, mutant ribosomes (named Spur)[21] and is used as a positive control. (**c**) Growth measurements of the Δ7*rrn* strain containing rDNA plasmid with MS2 tags at different positions and a non-tagged plasmid (WT, wild-type) as a sole source of rRNA. Average values are from three independent experiments (n = 3). Change in the growth rate of tagged plasmids as compared to non-tagged plasmid is ±5%.

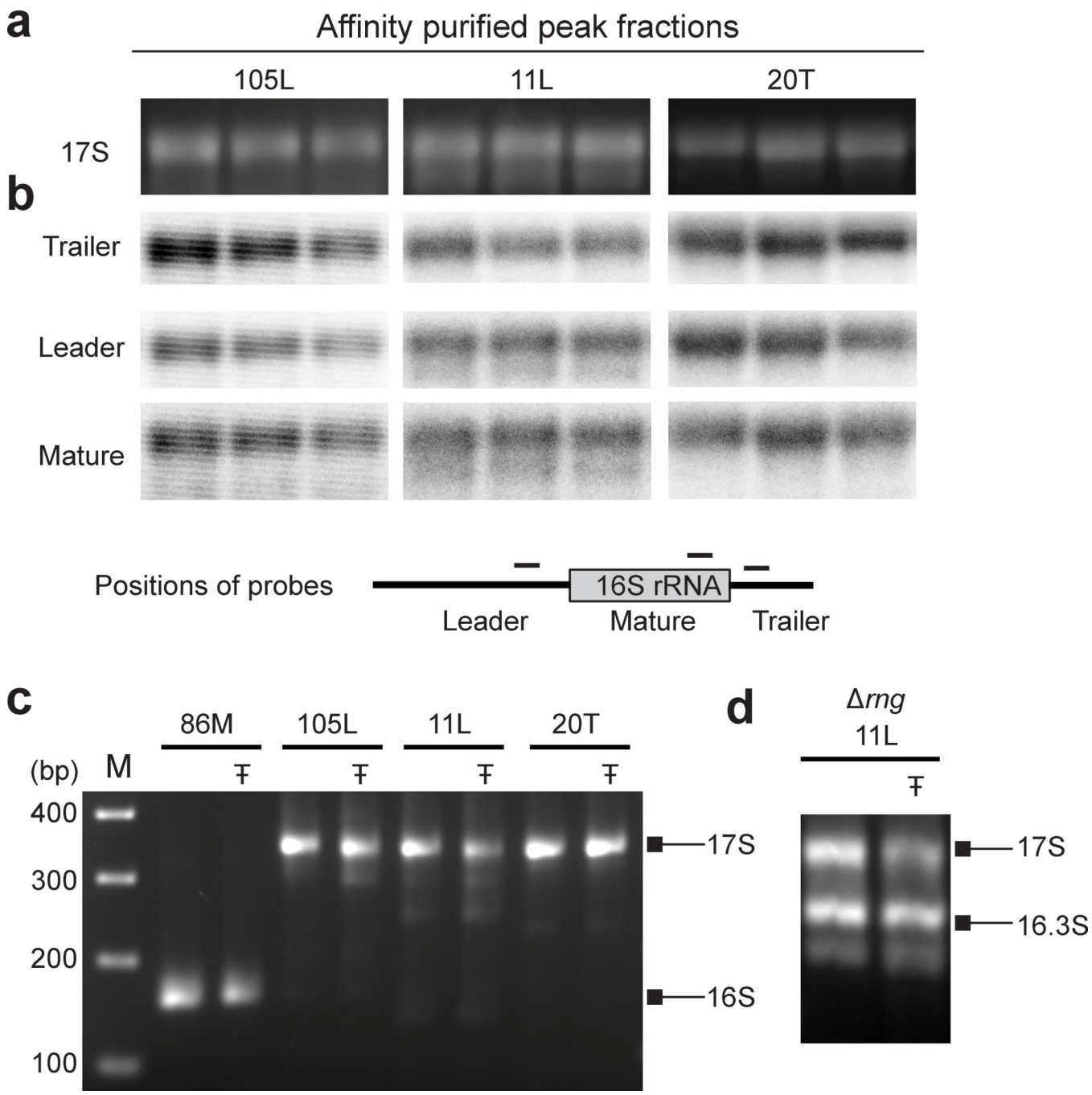

Figure 2. SSU intermediates purified with all three tags contain 17S rRNA as a major pre-16S rRNA species

(**a**) RNA analysis of rRNA purified with tags 105L, 11L and 20T on a 2% denaturing agarose gel stained with ethidium bromide. The three elution fractions with highest amounts of RNA from representative affinity purification are shown. Uncropped images are shown in Supplementary Data Set 3. (**b**) Northern blot analysis using probes directed to leader, trailer and mature regions of 16S rRNA for the same fractions as in Panel a. Positions of the probe are indicated below. Uncropped images are shown in Supplementary Data Set 3. (**c**) RT-

PCR (Reverse Transcription – Polymerase Chain Reaction) products of the ligated junctions of pre-16S rRNA purified with the three tags (modified 3′5′RACE; see Methods) resolved on a 2% agarose gel and stained with ethidium bromide. Only one fraction from the above analysis is shown; similar results are obtained for all elution fractions. ∓ indicates heat treatment of RNA before ligation. The experiments in panel a, b and c were carried out at least four times.(**d**) Modified 3′5′ RACE products of pre-16S RNA purified with tag 11L from the Δ*rng* strain of *E. coli*, which has been previously shown to accumulate 16.3S rRNA species, processed by RNase E at the 5′ end[13]. 16.3S rRNA is marked. Uncropped image is shown in Supplementary Data Set 3. The identity of the products is confirmed by sequencing (data not shown). The experiments were carried out two times.

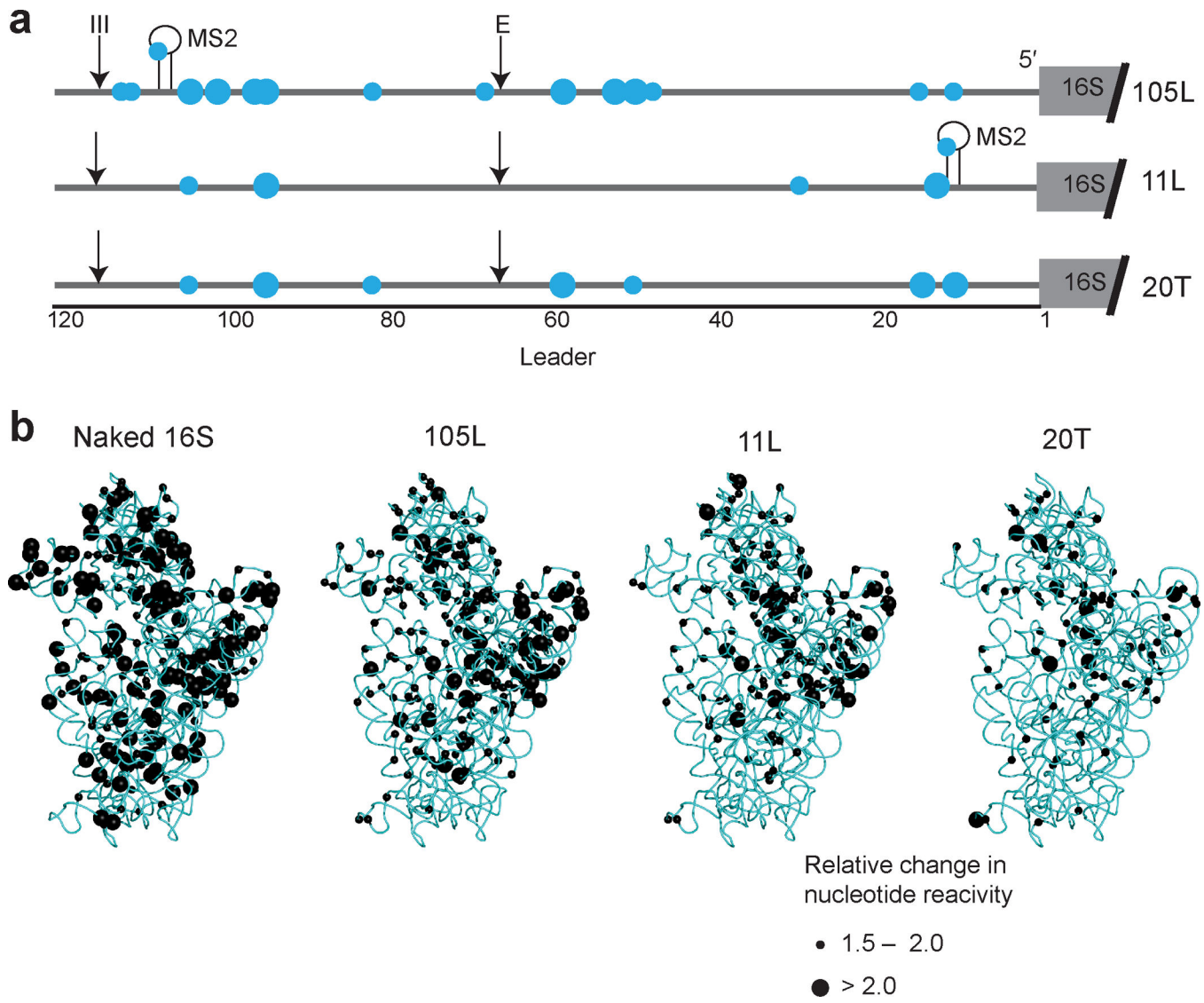

Figure 3. Distinct architecture of the three purified SSU assembly intermediates

(**a**) Altered nucleotide reactivity of leader in the three purified pre-SSU intermediates, as revealed by kethoxal probing, is classified as strong (large circle) and weak (small circle). Hairpin indicates the position of the MS2 tag. (**b**) Nucleotides with the altered reactivity in three pre-SSU 17S rRNA containing complexes purified with different tags and mature, naked 16S rRNA (r-proteins are removed) are shown on the three-dimensional crystal structure of the SSU (all r-proteins are omitted for clarity) (PDB: 2AVY)[34]. The relative changes in the nucleotide reactivity intensity of the intermediates and naked 16S rRNA (referred as the starting point in biogenesis process) are calculated relative to mature SSUs reactivity (as baseline; see Methods, Supplementary Fig. 3, Supplementary Data Set 1) and plotted as circles. Three independent biological replicates were performed; the nucleotides showing consistent changes in at least two experiments are shown. Residues with > 50% changes relative to mature SSUs are shown. The figures are generated using PyMol (http://www.pymol.org/).

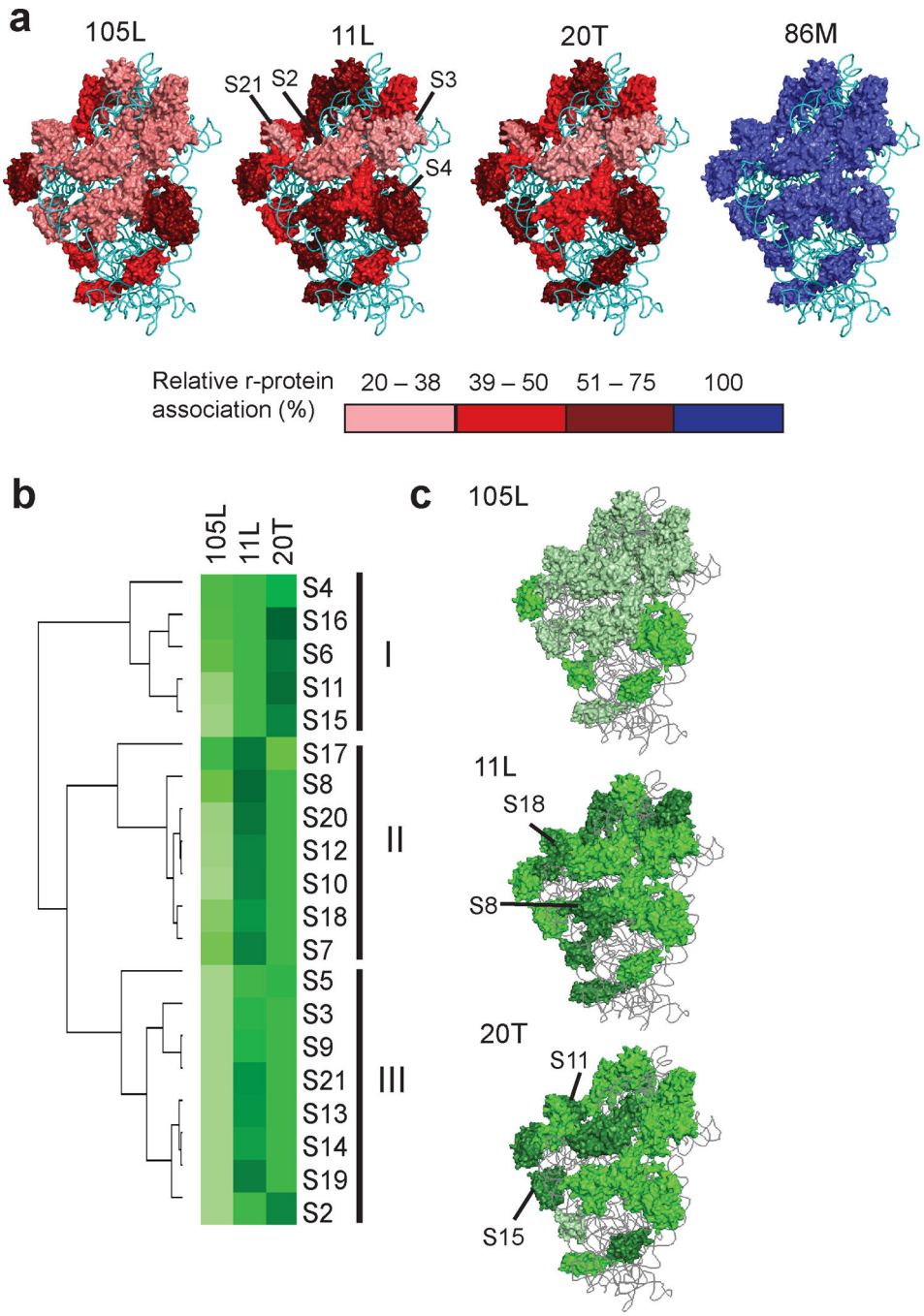

Figure 4. Multiple pathways for ribosomal proteins addition to the three intermediates

(**a**) Spectral counts of r-proteins bound to intermediates are compared to mature ribosomes purified with tag at position 86M (see Methods, Supplementary Data Set 2) and relative r-protein levels are calculated as percentages [biological replicates (n = 3) and technical replicates (n = 2)]. R-protein percentages of each intermediate are binned into 4 groups and plotted as heat maps on the three-dimensional crystal structure of SSU (PDB: 2AVY)[34]. Solvent side is shown (see Supplementary Fig. 4a for interface side). **(b)** Hierarchical clustering analysis of r-proteins bound to the 105L, 11L, and 20T tagged intermediates.

Relative protein abundance (RPA) for each r-protein present in each of the three SSU intermediates (but not mature SSUs) is calculated as described in Methods. Different shades of green indicate the levels of occupancy by a specific r-protein among the intermediates. The darker the green color, the more abundant the r-protein is bound in that intermediate as compared to the other intermediates. The r-proteins are clustered into three major groups, marked as I, II and III. (**c**) RPA of r-proteins associated with three intermediates is plotted on the three dimensional crystal structure of SSU (PDB: 2AVY)[34], 180° rotation shown. Colors are in as (b) and several r-proteins are labelled for reference. Solvent surface is shown (see Supplementary Fig. 4b for interface surface).

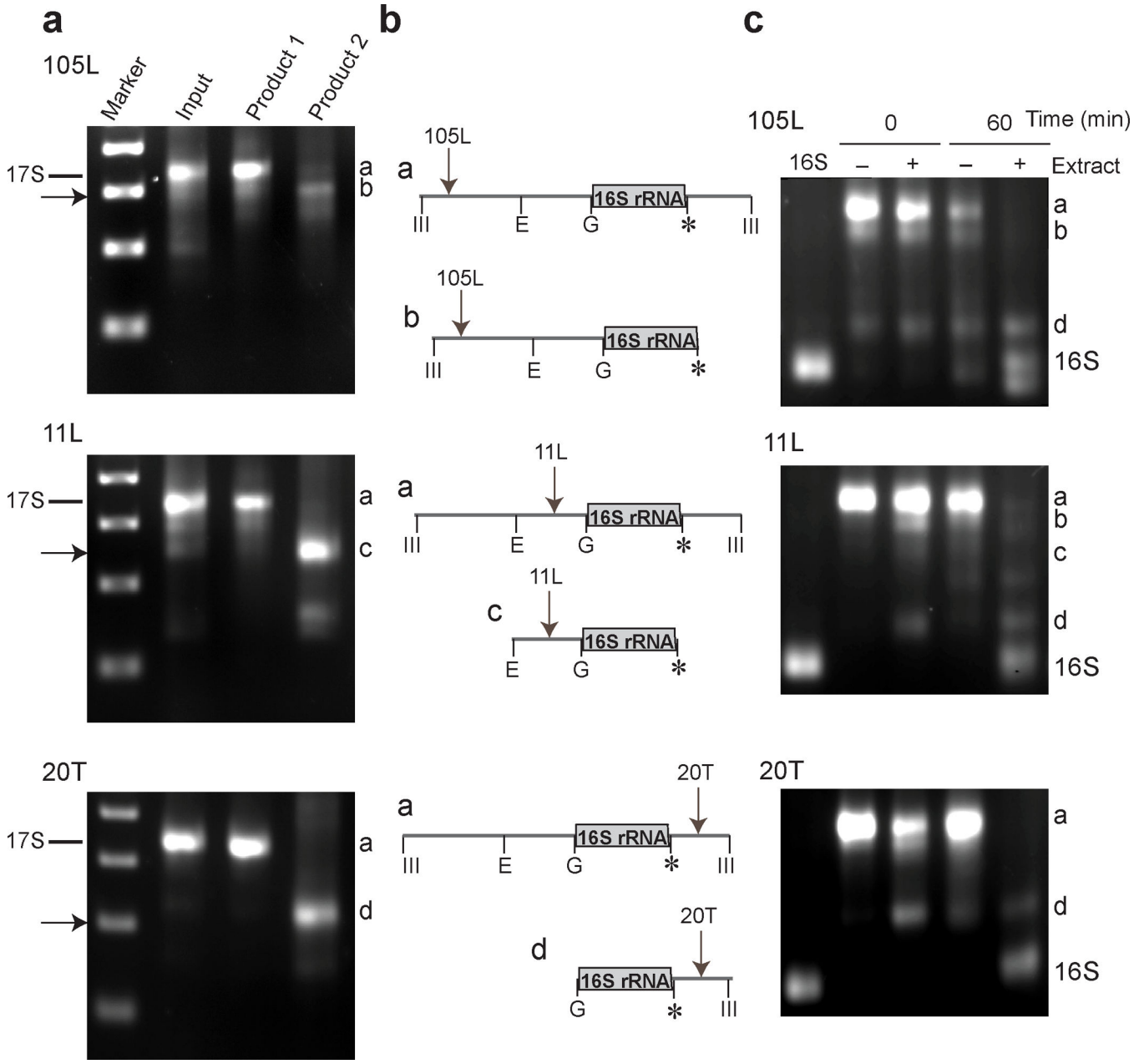

Figure 5. Maturation of 17S rRNA can initiate either at the 5′ or 3′ ends *in vivo* and *in vitro*

(**a**) Modified 3′5′ RACE products from the three purified intermediates separated on a 2% agarose gel. Intermediate pre-16S rRNA species are indicated by an arrow and is observed in all purifications (n > 10). 17S rRNA and intermediate pre-16S rRNA are gel purified and PCR amplified and products are resolved on a 2% agarose gel marked as Product 1 and Product 2. (**b**) Sequencing results of the various pre-16S rRNA processing species associated with the three different purified SSU intermediates products, each product is given a designation (a–d). The experiments were carried out two times. (**c**) Modified 3′5′ RACE products that result from incubation of the purified 105L, 11L and 20T assembly intermediates with wild-type extracts for 0 and 60 minutes (*in vitro*). '+' lanes indicate

addition of S100 and incubation time (in mins) is shown. The experiments were carried out three times. Uncropped image is shown in Supplementary Data Set 3. Various pre-16S rRNA species are marked as in Panel b.